

## **SUPPLEMENTARY INFORMATION**

### **S1. Additional information on statistical analysis**

Nannofossil data from the Cicogna section (NE Italy) were subjected to statistical analysis using the program PAST.

For PCA analysis, we additionally provide the biplot and the loading graphs of Component 1 and Component 2 (**Figure S1**).

For non-metric MultiDimensional Scaling (MDS) analysis, the species counts were combined to produce a matrix of 15 genera. A square root transformation, used to standardize the matrix, was chosen to minimize the influence of dominant taxa on the ordination (Schneider et al., 2011). Non-metric multidimensional scaling (MDS), using the Bray–Curtis distance metric (**Figure S2**) was applied in order to avoid assumptions as much as possible and guarantee the preservation of the relative differences between the samples (McCune and Grace, 2002).

### **References**

- Schneider L.J., Bralower, T.J., Kump, L.R.: Response of nannoplankton to early Eocene ocean deoxygenation, *Palaeogeogr., Palaeoclimatol., Palaeoecol.*, 310, 152-162, 2011.
- McCune, B., Grace, J.B.: *Analysis of Ecology Communities*. MjM Software Design, Gleneden Beach, Oregon, 2002.

### **S2. Further explanation regarding biostratigraphic calcareous nannofossil counts**

The high abundance, widespread distribution and rapid evolution of calcareous nannofossils make them one of the most powerful tool to date Cenozoic marine sediments. The use of semi-quantitative counting and the gathering of high resolved datasets greatly enhance their correlation potential (Backman et al., 2012; Agnini et al., 2014).

The methodology used in this study for samples of ODP Site 1262 is that proposed by Backman and Shackleton (1983), which consists in counting the number of calcareous nannofossils belonging to a specific taxon present in a prefixed area (1 mm<sup>2</sup>). Because of significant dilution by terrigenous material in samples from the Cicogna section, we extended the study area to 9 mm<sup>2</sup>. To further

appreciate the importance of semi-quantitative estimates and high-resolution sampling, we compare the Top *D. multiradiatus* and Base *D. lodoensis* as recorded from the Cicogna section, ODP Site 1262 and DSDP Site 550 (**FigureS3**). At Cicogna and ODP Site 1262, we provide detailed abundance patterns of these two taxa. *Discoaster multiradiatus* shows a first decrease in abundance preceding the H1 event and a definitive disappearance just before the onset of the I1 event. *Discoaster lodoensis* displays a first presence in the I1 event, which is followed by an interval of absence that eventually leads to its continuous and common presence close to the onset of the X event (**Figure S3**). Datasets from the Cicogna section and ODP Site 1262 allow a very detailed characterization of these two biohorizons and the recognition of peculiar features that are not present in the low-resolution qualitative biostratigraphic data available for DSDP Site 550. As a consequence, the stratigraphic position of Top *D. multiradiatus* and Base *D. lodoensis* at DSDP Site 550 are inaccurate. We hope that this simple exercise could serve to emphasize the crucial importance of producing high-resolution semi-quantitative data to obtain the most reliable biostratigraphic results.

## References

- Ali, J. and Hailwood, E.: Magnetostratigraphic (re)calibration of the Paleocene/Eocene boundary interval in Holes 550 and 549, Goban Spur, eastern North Atlantic, Earth Planet. Sci. Lett., 161, 201-213, 1998.
- Agnini, C., Fornaciari, E., Raffi, I., Rio, D., Röhl, U., and Westerhold, T.: High-resolution nannofossil biochronology of middle Paleocene to early Eocene at ODP Site 1262: implications for calcareous nannoplankton evolution. Mar. Micropaleontol., 64, 215-248, doi:10.1016/j.marmicro.2007.05.003, 2007b.
- Agnini, C., Fornaciari, E., Raffi, I., Catanzariti, R., Pälike, H., Backman, J., and Rio, D.: Biozonation and biochronology of Paleogene calcareous nannofossils from low and middle latitudes, Newslett. Stratigr., 47, 131-181, doi:10.1127/0078-0421/2014/0042, 2014.
- Backman, J., Raffi, I., Rio, D., Fornaciari, E. and Pälike, H., 2012: Biozonation and biochronology of Miocene through Pleistocene calcareous nannofossils from low and middle latitudes, Newslett. Stratigr., 45, 221-244.
- Cramer, B. S., Wright, J. D., Kent, D. V., and Aubry, M.-P.: Orbital climate forcing of  $\delta^{13}\text{C}$  excursions in the late Paleocene–early Eocene (Chronos C24n–C25n), Paleoceanography, 18 (4), 1097, doi:10.1029/2003PA000909, 2003.

- Dallanave, E., Agnini, C., Muttoni, G., and Rio, D.: Magneto-biostratigraphy of the Cicogna section (Italy): implications for the late Paleocene-early Eocene time scale, *Earth Planet. Sci. Lett.*, 285, 39-51, doi:10.1016/j.epsl.2009.05.033, 2009.
- Müller, C.: Biostratigraphic and paleoenvironmental interpretation of the Goban Spur region based on a study of calcareous nannoplankton, *Deep Sea Drill. Project, Initial Rep.*, 80, 389-414, 1985.
- Westerhold, T., Röhl, U., Raffi, I., Fornaciari, E., Monechi, S., Reale, V., Bowles, J., and Evans, H. F.: Astronomical calibration of the Paleocene time, *Palaeogeogr. Palaeoclimatol. Palaeoecol.*, 257, 377-403, doi:10.1016/j.palaeo.2007.09.016, 2008.
- Zachos, J. C., Kroon, D., Blum, P., et al.: Early Cenozoic Extreme Climates: The Walvis Ridge Transect, *Proc. Ocean Drill. Program, Initial Rep.*, 208 doi:10.2973/odp.proc.ir.208.2004, 2004.

### **S3. Looking through “frosty glass”: Comparison to records at ODP Site 690**

We have presented fairly detailed records of bulk carbonate  $\delta^{13}\text{C}$  and quantified calcareous nannofossil assemblages for the lower Paleogene section at Cicogna, and compared these records with those at the only two locations with similar information. From this comparison, we suggest that a very detailed template exists for the alignment of  $\delta^{13}\text{C}$  records and calcareous nannofossil assemblage counts across the early Paleogene (**Figure 11**), one with much higher resolution than given in most previous work, and one most likely related to changes in past global carbon cycling, oceanography, and calcareous nannoplankton evolution.

Significant variations in calcareous nannofossil abundances definitely happened at multiple locations during the PETM (Bralower, 2002, and references noted in main text). However, it is by no means clear whether such changes extended across the broader early Paleogene, nor how such changes might compare to those across the PETM. One can certainly speculate that variations in calcareous nannofossil abundance records and bulk carbonate  $\delta^{13}\text{C}$  records might correlate in fine temporal detail across widely distributed sites throughout the early Paleogene, given well-established calcareous nannofossil biozone schemes (Martini, 1971; Okada and Bukry, 1980; Agnini et al., 2014), and a growing appreciation of a very dynamic carbon cycle over this time interval. Nonetheless, the generation of detailed and coupled multi-million year records for quantified calcareous nannofossil abundances and bulk carbonate  $\delta^{13}\text{C}$  perplexed one of the referees for this

paper, who insisted that we needed to make comparisons with existing work at ODP Site 690 and to explain discrepancies.

The lower Paleogene record at Site 690 provides a very good example in which to highlight the basic background and importance of our work. Three holes were drilled and cored at ODP Site 690 on Maud Rise (South Atlantic; Figure 1) in 1987 using the advanced piston corer (APC) (Barker et al., 1988). Sediment recovery within each core was nearly 100 %, although some cores were shorter than the full 9.7 m. However, most of the lower Paleogene sequence was retrieved in only one of the holes, 690B (Barker et al., 1988). This is important, because m-scale gaps generally occur between successive cores during APC operations (Ruddiman et al., 1987; Lisiecki and Herbert, 2007). The early Paleogene section at Site 690 is, almost assuredly, incomplete, with “missing” portions at each core break.

Sediment from Core 690B-19H has been the focus of numerous papers, as it contains the PETM (Kennett and Stott, 1991; Bains et al., 1999; Bralower, 2002). However, correlating this core to the surrounding sedimentary record at Site 690, and the latter to early Paleogene records at other locations is problematic, at least with any detail. For example, using Hole 690B records, Cramer et al. (2003) estimated that 1.4 Myr occurred between the PETM and the H-1 event. This is incorrect, as the duration is close to 1.8 Myr (Westerhold et al., 2008). Beyond the aforementioned core gaps, there are major issues with the paleomagnetic record of early Paleogene sediments in Hole 690B (Ali et al., 2000). Indeed, Ali et al. (2000) recommend using calcareous nannofossil records for correlation purposes of this interval.

Records of bulk carbonate  $\delta^{13}\text{C}$  (Cramer et al., 2003) and calcareous nannofossil relative abundances (Pospichal and Wise, 1990) have been generated using sediment at Hole 690B. When coupled together (**Figure S4**), these records show similarities to those at Cicogna (**Figure 11**). There is the long-term late Paleocene-early Eocene drop in  $\delta^{13}\text{C}$  and several superimposed short-term

negative CIEs. There are also closely coeval changes in calcareous nannofossil abundances, such as the peak in *D. multiradiatus* across the C event, the subsequent peak in *Fasciculithus* spp., and the cross-over of *T. contortus* and *T. orthostylus* just before the H-1 event. One can also see the problem with examining nannofossils at low depth/time resolution and qualitatively. We suggest here a “frosty glass” hypothesis, where details of Earth system change in the distant past are blurred presently by poorly resolved stratigraphy. This includes basic problems with aligning sections in depth and time, as well as interpretable quantification of data at high spatial resolution. Despite the need for additional work at Site 690, we suggest that available records at this location support the template offered in the main text.

## References

- Agnini, C., Fornaciari, E., Raffi, I., Catanzariti, R., Pälike, H., Backman, J., and Rio, D.: Biozonation and biochronology of Paleogene calcareous nannofossils from low and middle latitudes, *Newslett. Stratigr.*, 47, 131-181, doi:10.1127/0078-0421/2014/0042, 2014.
- Ali, J. R., Kent, D. V., and Hailwood, E. A.: Magnetostratigraphic reinvestigation of the Palaeocene/Eocene boundary interval in Hole 690B, Maud Rise, Antarctica, *Geophys. J. Int.*, 141 (3), 639-646, doi: 10.1046/j.1365-246X.2000.00109.x, 2000.
- Bains, S., Corfield, R. M. and Norris R. D.: Mechanisms of climate warming at the end of the Paleocene, *Science*, 285, 724-727, 1999.
- Barker, P.E, Kennett, J.P., et al.: *Proc. ODP, Init. Repts.*, 113, 1-774, doi:10.2973/odp.proc.ir.113.1988, 1988.
- Bralower, T. J.: Evidence of surface water oligotrophy during the Paleocene–Eocene thermal maximum: nannofossil assemblage data from Ocean Drilling Program Site 690, Maud Rise, Weddell Sea, *Paleoceanography*, 17, 1029-1042, doi:10.1029/2001PA000662, 2002.
- Cramer, B. S., Wright, J. D., Kent, D. V., and Aubry, M.-P.: Orbital climate forcing of  $\delta^{13}\text{C}$  excursions in the late Paleocene-early Eocene (Chronos C24n–C25n), *Paleoceanography*, 18 (4), 1097, doi:10.1029/2003PA000909, 2003.
- Kennett, J. P. and Stott, L. D.: Abrupt deep-sea warming, palaeoceanographic changes and benthic extinctions at the end of the Palaeocene, *Nature* 353, 225-229 doi:10.1038/353225a0, 1991.
- Lisiecki, L. E., and Herbert, T. D.: Automated composite depth scale construction and estimates of sediment core extension, *Paleoceanography*, 22(4), PA4213, doi:10.1029/2006PA001401, 2007.

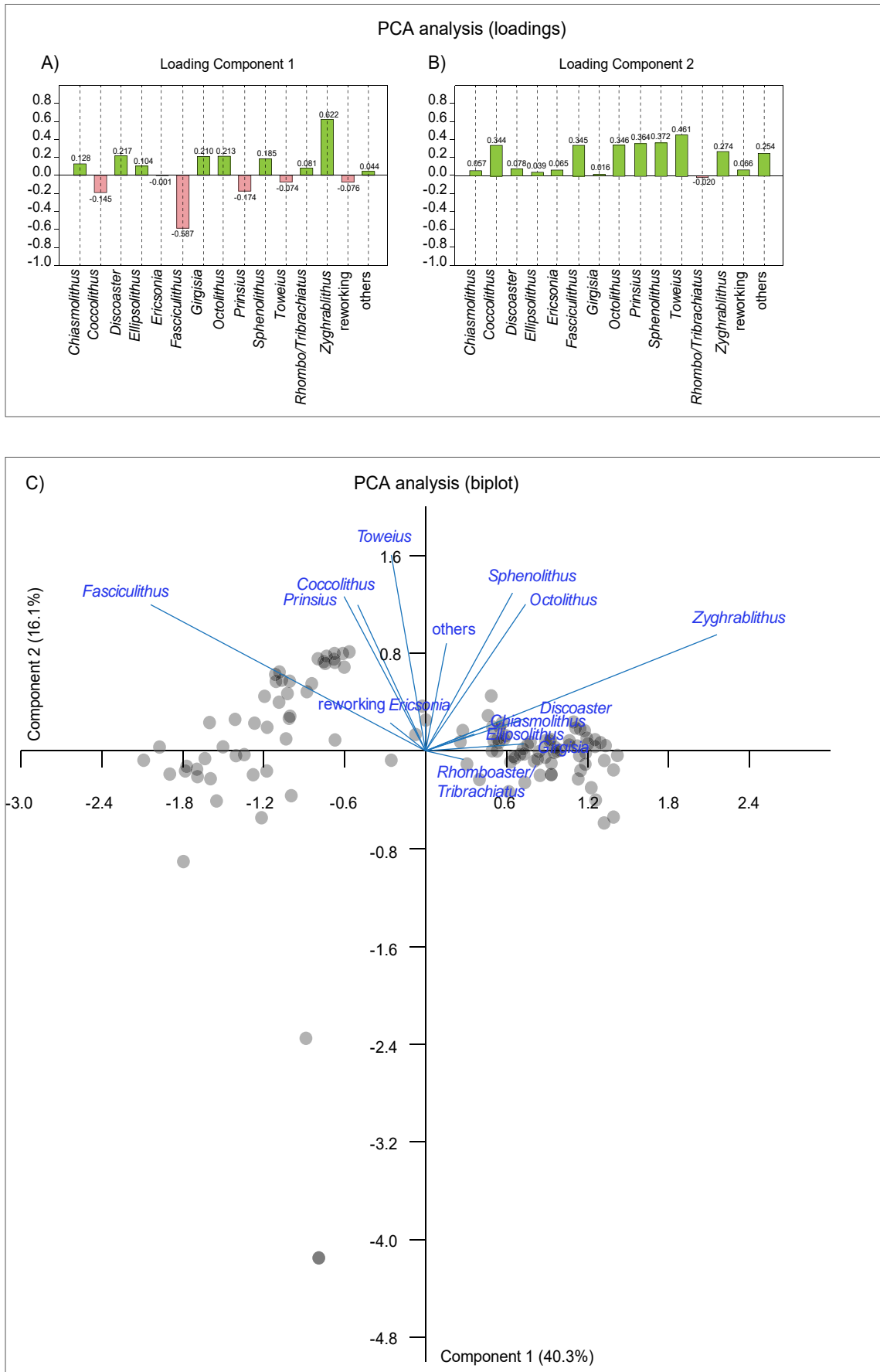
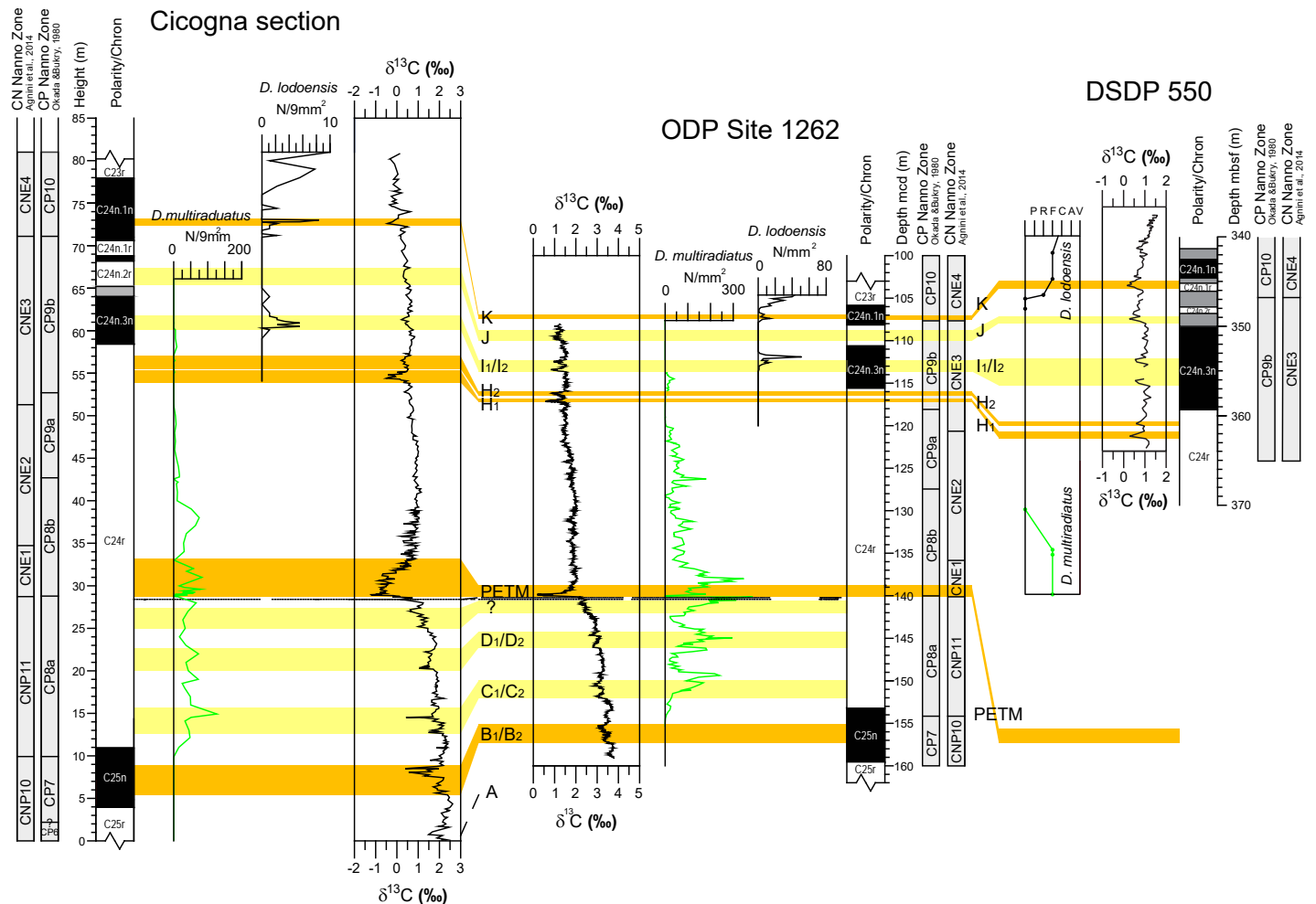


Figure S1. PCA plots of calcareous nannofossil data from the Cicogna section (Italy). A) Loading plot of Component 1; B) Loading plot of Component 2; C Biplot.

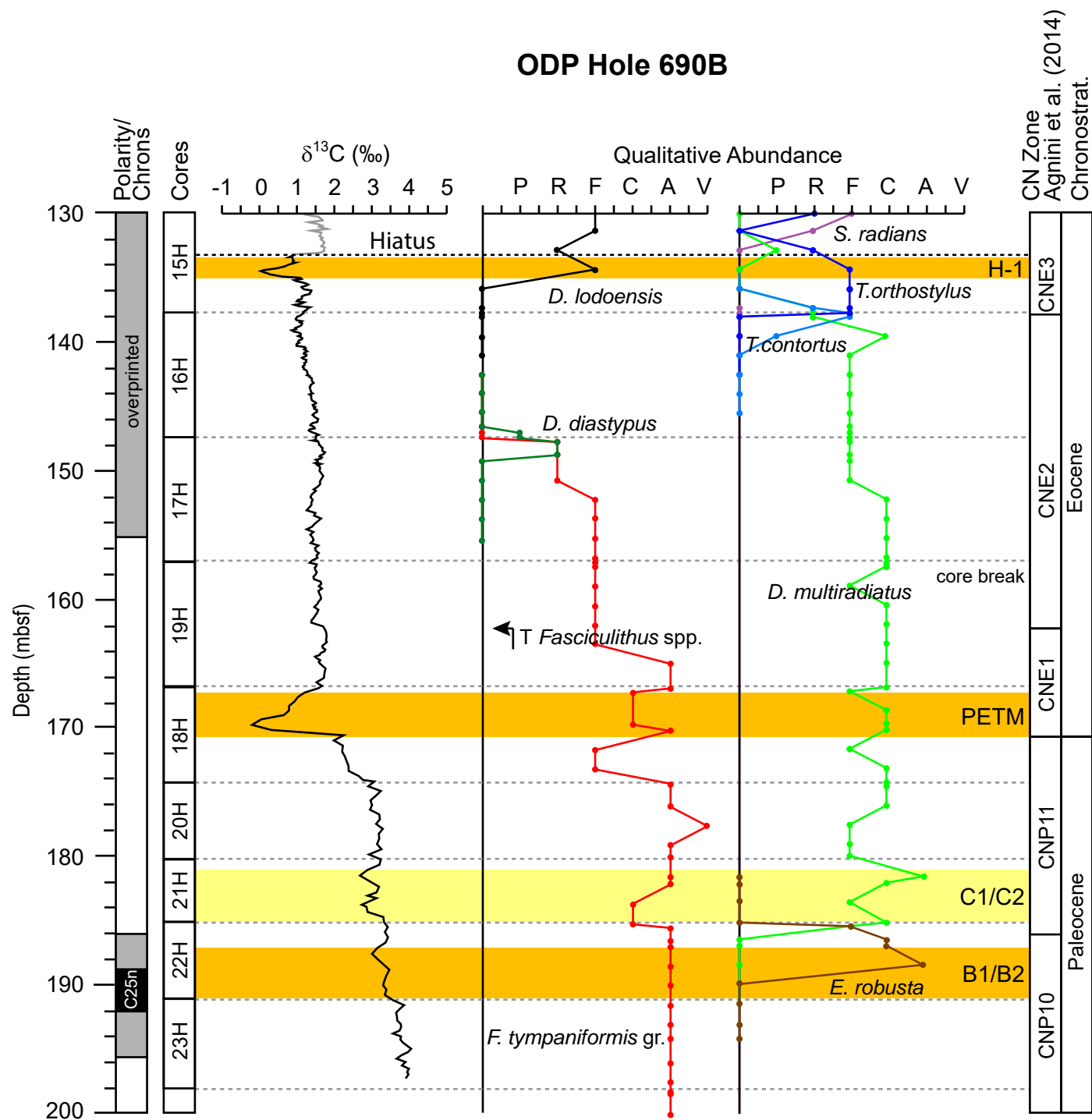
PCA plot showing the distribution of 180 samples across three geological stages: PETM (red), Eocene (blue), and Paleocene (green). The x-axis is labeled 'Coordinate 1' and the y-axis is labeled 'Coordinate 2'. The plot includes a legend identifying sample types: Paleocene samples (green), B1/B2 events (yellow), Eocene samples (black), PETM CIE core (red), PETM CIE recovery (orange), H1/H2 events (blue), and K event (purple). The PETM cluster is centered around (-0.15, 0.08), the Eocene cluster around (0.05, 0.08), and the Paleocene cluster around (-0.05, -0.05). The K event (purple) is located near the boundary between PETM and Eocene. The B1/B2 events (yellow) are located near the boundary between Eocene and Paleocene. The H1/H2 events (blue) are located near the boundary between Eocene and Paleocene. The PETM CIE core (red) and PETM CIE recovery (orange) are located near the boundary between PETM and Paleocene. The Eocene samples (black) are located near the boundary between Eocene and Paleocene. The Paleocene samples (green) are located near the boundary between Paleocene and Eocene. The B1/B2 events (yellow) are located near the boundary between Eocene and Paleocene. The H1/H2 events (blue) are located near the boundary between Eocene and Paleocene. The K event (purple) is located near the boundary between PETM and Eocene.

Figure S2. Non-metric multidimensional scaling (MDS) plot of calcareous nannofossil data from the Cicogna section (Italy). Grey dots = barren to virtually barren samples (see supplementary information for details).



**Figure S3.** Abundance patterns of *D. multiradiatus* and *D. lodoensis* from the Cicogna section, ODP Site 1262 and DSDP Site 550. For these three successions paleomagnetic (Ali and Hailwood, 1998; Dallanave et al., 2009; Westerhold et al., 2008), carbon isotope (Cramer et al., 2003; Zachos et al., 2004; this study) and calcareous nannofossil data (Müller, 1985; Agnini et al., 2007, this study) are available. Top *D. multiradiatus* and Base *D. lodoensis* are clearly recognizable at Cicogna and ODP Site 1262, where quantitative counts have been performed. By contrast, qualitative data from DSDP Site 550 do not provide reliable biostratigraphic data P= present; R=rare; F=few; C=common; A=abundant; V=very abundant.





**Figure S4.** Carbon isotope data from ODP Site 690 (Cramer et al., 2003) plotted against qualitative abundance estimates of selected calcareous nannofossil taxa (Pospichal and Wei, 1990). Top *Fasciculithus* spp. (Aubry et al., 1996).